Phase closure in optical astronomy

Fermeture de phase en astronomie optique

Nigel R. ARNOT

Department of Physics, Queen Elizabeth College, Campden Hill Rd., LONDON W8 7AH, UK

Mr. Arnot Graduated in 1979 from Trinity College, Cambridge and initially worked at Queen Elizabeth College on the analysis of electron images. Some work on the phase problem and ambiguities in image reconstruction from transform modulus information led into problems associated with astronomical imaging, and he is currently preparing A Ph. D. Thesis which will centre about the techniques described in this paper.

Paul D. ATHERTON

Kapteyn Laboratorium, Rijksuniversiteit te Groningen, Postbus 800, 9700 AV, GRONINGEN, The Netherlands

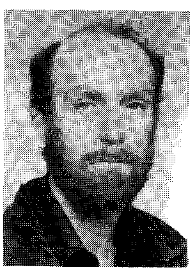

Alan H. GREENAWAY

Centre for Theoretical Studies, RSRE, St. Andrews Rd., MALVERN, WR14 3PS, UK

Since finishing A Ph. D. on electron microscopy in 1976, DR. Greenaway has worked on inverse problems, primarily in the field of optics, at the universities of Groningen (NL), London (U.K.) and Nice (France). He has worked at R.S.R.E. since 1982, With emphasis on the problems of imaging through turbulence.

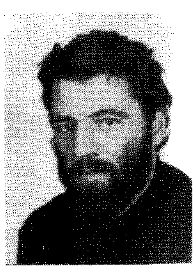

Jan E. NOORDAM

Royal Greenwich Observarory, Herstmonceux Castle, E. Sussex, BN27 1RP, UK (permanent address: Netherlands Foundation for Radio Astronomy, DWINGELOO, The Netherlands).

Physics degree from Technische Hoogeschool from 1975, Jan E. Noordam is working for Westerbork Radio Delf, Telescope on problems in Radio Aperture Synthesis. From 1983 on loan to Royal Greenwich Observatory (England) to help with the new ground optical observatory on La Palma in the Canary Islands.

SUMMARY

Simplifications of recently proposed techniques for using phase closure to achieve diffraction-limited imaging in optical astronomy are considered.

The technique permits synthesis of diffraction-limited images from single, short-exposure, turbulence-degraded images of bright objects viewed through the earth's atmosphere, but is more important as a method for obtaining high resolution images from earth-orbit without the need to put a single large aperture of accurate figure in space.

The basis of the method is a multi-aperture interferometer with sufficient redundancy built into the instrument to permit the separation of instrumental and object dependent parameters and thus to permit each of these to be determined without recourse to model building.

By use of image-slicing and optical delay lines it is possible to achieve broad-band imaging in two sub-fields. One of the sub-fields may be used as a reference to "shape lock" the instrument to $\lambda/100$ accuracy on a source of magnitude $\lesssim 12$, whilst the other is used to obtain long integrations on faint objects.

KEY WORDS

Astronomy, interferometer, Fourier, shape lock.

RÉSUMÉ

On envisage des simplifications aux techniques récemment proposées afin d'utiliser la « fermeture de phase » en astronomie optique, techniques visant à obtenir la limite théorique de diffraction en imagerie.

La méthode envisagée permet de corriger des images isolées, obtenues à courte exposition et dégradées par la turbulence atmosphérique, jusqu'à la limite de diffraction malgré la traversée de l'atmosphère terrestre. Elle prend toute son importance lorsqu'on l'applique à obtenir des images de haute résolution à partir d'une orbite autour de la Terre sans qu'il soit nécessaire de disposer à bord du satellite d'une surface de haute précision optique sur une grande ouverture.

A la base de cette méthode : un interféromètre à pupilles multiples, comportant suffisament de redondances internes pour pouvoir séparer les paramètres de l'objet de ceux de l'instrument, chacun étant déterminé alors sans introduire de modèles a priori.

Pour une application spatiale, le champ pourrait être dédoublé au moyen de séparateurs et de retards optiques autorisant des mesures à large bande. Une source de référence permet alors dans l'un des champs la stabilisation active de l'instrument — une précision de 1/100 de longueur d'onde paraît accessible, en étudiant une configuration praticable, sur une étoile de magnitude inférieure a 12. L'autre champ est alors disponible pour de longues intégrations sur des objects faibles.

MOTS CLÉS

Astronomie, Interferométrie, Fourier, Diffraction.

CONTENTS

1. Introduction

The principle of synthesising an image of a self-luminous object by making measurements of its mutual coherence function, rather than by direct imaging, is well known in the context of radio astronomy. Such image synthesis generally relies, explicitly or implicitly, on model building to obtain a multi-parametric fit to the measured data. The best of these techniques (e. g. "self-calibration" applied to non-redundant arrays like the VLA [1]) work fairly well because the number of parameters to be fitted only marginally exceeds the volume of available data and can often be fitted using *a priori* information (e. g. source size and positivity). Clearly, the smaller the excess number of parameters relative to the volume of data, the better one would expect such procedures to work. Building redundancy into the measurements permits one to reduce the number of parameters to be fitted. Indeed, sufficient redundancy may be built into the instrument to give an overdetermined system, in which case a least squares solution may be obtained to minimize errors without recourse to the use of models. The proposal to use redundancy in such a formal way in order to obtain model independent solutions was made in 1982 in the context of both radio astronomy [2] and optical astronomy [3]. It has already been demonstrated in radio astronomy [2] that application of the principle of redundant calibration leads to an ability to synthesise very high dynamic range images, without the need to invoke source models or use iterative techniques. The application of this principle in optics is still at the proposal stage, but progressive changes in optical design [4, 5] have greatly improved the signal to noise whilst at the same time simplifying the optics. The result is an instrument that has much in common with radio aperture synthesis arrays.

Although redundant calibration may be used to compensate for atmosheric turbulence in terrestial observations, its most important application is lilely to be for Optical Aperture Synthesis In Space (OASIS).

In this article, which is based on a paper presented at the *Data Signal and Image Processing Symposium* of the URSI General Assembly in Florence (September 1984), the principles of stellar interferometry and of aperture synthesis by phase closure will be reviewed. The modification of this technique to facilitate model independent image reconstruction, by using the principles of redundant calibration, will then be discussed. Finally, we shall review applications of this technique with particular reference to OASIS.

2. Principles of stellar interferometry

Consider a simple two-telescope stellar interferometer, in which the images of two starlight-illuminated apertures are brought to focus at a common point (*Fig.* 1). Just as in a Youngs-slit experiment, the intensity distribution in the detector plane will be modulated by a cosinusoidal fringe pattern whose contrast depends upon the degree of coherence between the light illuminating the two apertures. This fringe pattern may be characterised by two parameters, its visibility, $|\gamma|$, and its phase, θ. In an idealised situation, these parameters depend only upon the separation between the two apertures. Their relationship to the detected intensity distribution is shown in Figure 2.

The complex function:

$$\gamma(\xi)=|\gamma(\xi)|\exp[i\,\theta(\xi)], \tag{1}$$

formed by changing the spatial frequency ξ (aperture separation measured in wavelength units), is referred to as the complex degree of coherence. By the van Cittert-Zernike theorem [6], $\gamma(\xi)$ is the normalized Fourier transform of the brightness distribution of the stellar source that is illuminating the apertures. Thus, in principle, one could reconstruct the object under study by measuring $\gamma(\xi)$ using a pair of apertures of vaying separation and then taking the inverse Fourier transform in a computer.

If one tried to use this simple scheme to measure $\gamma(\xi)$ one would find that atmospheric turbulence or mechanical instabilites introduce random phase shifts into the two beams. The result of such shifts is to displace the fringe pattern in the detector plane, i. e. to change the phase of the fringes. Clearly, if the displacement of the fringe pattern during the detector integration time is significant compared to the fringe crest spacing, the detector will register an averaged fringe pattern of reduced (perhaps zero) contrast.

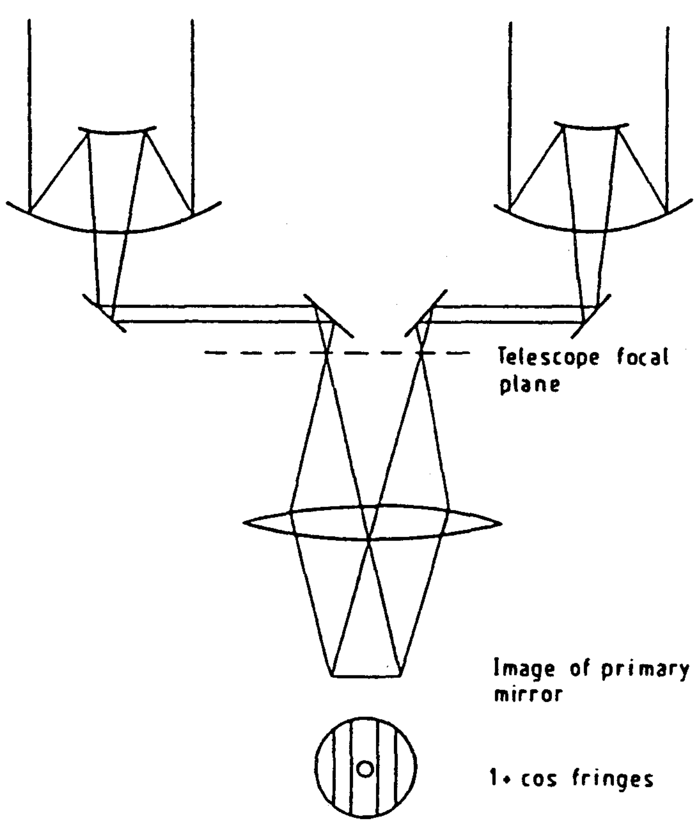

Fig. 1. — A simple two-aperture interferometer.

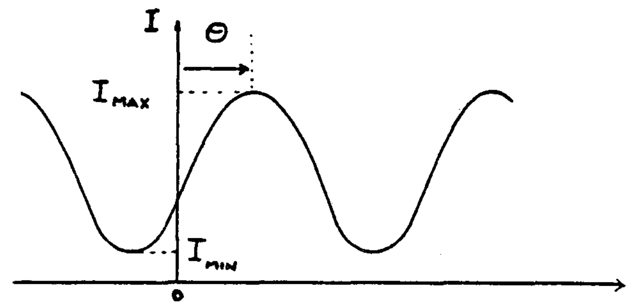

Fig. 2. — The detected intensity, showing fringe phase and the maximum and minimum intensity:

$$|\gamma|=\frac{I_{max}-I_{min}}{I_{max}+I_{min}}.$$

If the integration time is shortened to ensure that fringe movement during integration is negligible, one may measure the true fringe contrast but the phase of the fringes will be random, depending on the phase shifts in the two interferometer arms. For this reason such interferometers have been used to measure the modulus, but not the phase, of the object Fourier transform. Without the phase of the object Fourier transform one cannot, in general, unambiguously reconstruct the image of the object. Knowledge of only the modulus of the object Fourier transform yields only the autocorrelation of the object image, here the interest is in producing the image itself.

Since the problems discussed above have been encountered and largely solved in radio astronomy, where images of sources are now routinely made, it seems reasonable to apply radio astronomy techniques in optics as far as one can. Thus one should consider the phase closure method, by which same problem was solved in radio astronomy.

Before proceeding, several pertinent features of the simple interferometer of figure 1 should be commented upon.

Firstly, a convenient way of analysing the fringe pattern, to obtain the visibility and phase of the fringes, is to take the Fourier transform of the detected intensity distribution. This transform consists of three delta-like peaks, one at the origin in Fourier space and two symmetrically placed about that origin. The visibility of the fringes, calculated according to the formula given in the legend to Figure 2, is exactly twice the ratio of the height of one of the sideband peaks to the peak at the origin. The phase of the fringes is the phase of the complex number which appears as a weight for the sidebands.

Secondly, the period of the fringe pattern on the detector depends only upon the angle at which the two light beams are brought together, and this is entirely under the control of the instrument designer. Use will be made of this in the next section, where more apertures will be added to the interferometer and the angles at which the beams are brought together chosen to ensure that, in the resulting composite fringe pattern, each fringe period is uniquely identifiable with a specific pair of apertures. As before, the visibility and phase of each of the superposed sets of fringes are most conveniently found by Fourier transforming the detected pattern.

3. Phase closure aperture synthesis

Consider an interferometer with $N \geq 2$ apertures and in which the images of all of these apertures are brought to focus at the same point. With N apertures there are $N(N-1)/2$ different ways to choose a pair of apertures and, if the angles at which the beams intersect in the detector plane are carefully chosen, it may be arranged that no two pairs of beams intersect at equal angles. The detected intensity will then be modulated by $N(N-1)/2$ fringe patterns of differing fringe period. Since each aperture pair corresponds to a unique fringe period and each fringe period gives rise to two delta-like peaks in the Fourier space, every sideband in the Fourier spectrum may be identified with a given aperture pair and thus with a given spatial frequency.

The real breakthrough in radio astronomy came when it was realised that by using a large number of apertures one may simultaneously measure $\gamma(\xi)$ at many more values of ξ than there are unknown phase shifts in the interferometer arms. Thus it is possible to envisage a solution technique in which one tries to calculate the image of the object using the experimental data supplemented by *a priori* information about the object (e. g. it is of finite size and positive definite). To understand this consider a system of 4 apertures, Figure 3.

Let ξ_{jk} be the baseline between apertures j and k and let the complex gain associated with the j-th aperture be a constant g_j where:

$$g_j = |g_j| \exp(i\xi_j).$$

In general, $|g_j|$ would represent reflection losses etc and φ_j would represent path length errors associated with each aperture.

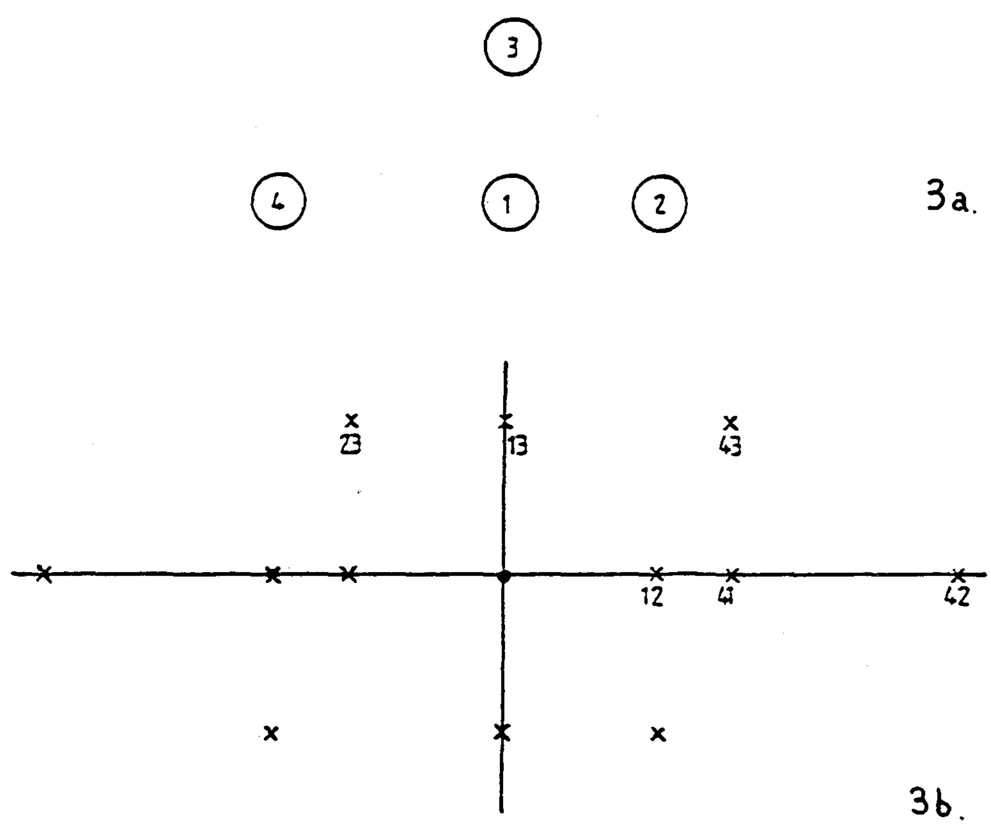

Fig. 3. — The four aperture interferometer discussed in the text. Figure 3*a*: The real-space relationship of the four apertures. Figure 3*b*: The spatial frequencies measurable with the aperture system of 3*a*.. Since the object is real $\gamma(\xi)$ has an Hermitian symmetry. Thus only six independent spatial frequencies (e. g. the numbered crosses) may be measured. The numbering represents the aperture pair involved in producing each spatial frequency. Each spatial frequency sideband has a weight of 0.25 relative to unity at the origin (solid circle).

Then the logarithm of the degree of coherence actually measured by Fourier transforming the detected fringe pattern may be written:

$$\begin{aligned}\ln[v(\xi_{jk})] &= a_{jk} + i b_{jk} \\ &= \ln[|\gamma(\xi_{jk})|] + \ln[|g_j|] + \ln[|g_k|] \\ &\quad + i[\theta(\xi_{jk}) + \varphi_j - \varphi_k]. \end{aligned} \tag{2}$$

Clearly, with N apertures one has $N(N-1)/2$ equations of form (2). For reasons that will become apparent later, it is convenient to consider the real and imaginary parts of (2) separately.

Consider, firstly, the imaginary parts of equations (2). There are $N(N-1)/2$ unknown θ-values and N unknown φ-values. However, specifying an arbitrary value for two $\theta(\xi)$ is equivalent to fixing an arbitrary position for the object on the sky. If one is interested only in the morphology of the object this is inconsequential. Further, in imaging only relative phases matter, thus one may arbitrarily choose one φ to be zero. Taking advantage of the disposable parameters available as a result of these θ and φ values, reduces the number of unknowns by three.

This still leaves a system of $N(N-1)/2$ equations in $(N+3)(N-2)/2$ unknowns. Even if all the equations are independent, such a system cannot be solved in closed form, except for the case $N=3$. This is the situation in a non-redundant system, i. e. one where:

$$\xi_{jk} \neq \xi_{lm}; \qquad \forall jk \neq lm.$$

To take a specific example, the 4-aperture system shown in Figure 3 gives rise to the matrix equation:

$$\begin{vmatrix} 1 & 0 & 0 & 0 & 0 & 0 & 1 & -1 & 0 & 0 \\ 0 & 1 & 0 & 0 & 0 & 0 & 1 & 0 & -1 & 0 \\ 0 & 0 & 1 & 0 & 0 & 0 & -1 & 0 & 0 & 1 \\ 0 & 0 & 0 & 1 & 0 & 0 & 0 & 1 & -1 & 0 \\ 0 & 0 & 0 & 0 & 1 & 0 & 0 & -1 & 0 & 1 \\ 0 & 0 & 0 & 0 & 0 & 1 & 0 & 0 & -1 & 1 \\ 0 & 0 & 0 & 0 & 0 & 0 & 1 & 0 & 0 & 0 \\ 1 & 0 & 0 & 0 & 0 & 0 & 0 & 0 & 0 & 0 \\ 0 & 1 & 0 & 0 & 0 & 0 & 0 & 0 & 0 & 0 \end{vmatrix} \times \begin{vmatrix} \theta_{12} \\ \theta_{13} \\ \theta_{41} \\ \theta_{23} \\ \theta_{42} \\ \theta_{43} \\ \varphi_1 \\ \varphi_2 \\ \varphi_3 \\ \varphi_4 \end{vmatrix} = \begin{vmatrix} b_{12} \\ b_{13} \\ b_{41} \\ b_{23} \\ b_{42} \\ b_{43} \\ 0 \\ 0 \\ 0 \end{vmatrix} \tag{3}$$

The first six equations in (3) correspond to the measurements at the six available spatial frequencies ξ_{jk}. The last three equations correspond to the choice of the value zero for the three disposable parameters (θ_{12}, θ_{13} and φ_1). There are an infinity of possible one parameter solutions correspond to solving equation (3) by back substitution using an arbitrary value for φ_4.

4. Principles of redundant calibration

In a redundant system one has:

$$\xi_{jk} = \xi_{lm} \qquad \text{for at least some } jk \neq lm,$$

and so two or more of the equations involve the same $\theta(\xi)$, thus the number of unknowns is reduced. The cost of this redundancy is a reduction in the number of spatial frequencies for which $\gamma(\xi)$ may be evaluated. In radio astronomy it is usual to use a non-redundant array to maximize the number of ξ-values available and to rely on *a priori* information to solve for the missing parameters. For example, 27 antennae are used in a non-redundant array in the case of the VLA and this leaves a 24 parameter solution for the imaginary parts of (2), since one has 351 equations in 375 unknowns. However, a rearrangement of the aperture configuration could provide 24 repeated baselines, thus reducing the number of unknowns to 351 and giving a closed form solution. Reducing the number of baselines from 351 to 327 would seem a small price to pay for this advantage.

Returning to the example of the aperture system of Figure 3, if the spacing between apertures 4 and 1 is the same as that between apertures 1 and 2, one has $\xi_{12} = \xi_{41}$. Thus one may write:

$$\theta_{12} - \theta_{41} = 0,$$

as an extra equation in (3), giving:

$$\begin{vmatrix} 1 & 0 & 0 & 0 & 0 & 0 & 1 & -1 & 0 & 0 \\ 0 & 1 & 0 & 0 & 0 & 0 & 1 & 0 & -1 & 0 \\ 0 & 0 & 1 & 0 & 0 & 0 & -1 & 0 & 0 & 1 \\ 0 & 0 & 0 & 1 & 0 & 0 & 0 & 1 & -1 & 0 \\ 0 & 0 & 0 & 0 & 1 & 0 & 0 & -1 & 0 & 1 \\ 0 & 0 & 0 & 0 & 0 & 1 & 0 & 0 & -1 & 1 \\ 0 & 0 & 0 & 0 & 0 & 0 & 1 & 0 & 0 & 0 \\ 1 & 0 & 0 & 0 & 0 & 0 & 0 & 0 & 0 & 1 \\ 0 & 1 & 0 & 0 & 0 & 0 & 0 & 0 & 0 & 0 \\ 1 & 0 & -1 & 0 & 0 & 0 & 0 & 0 & 0 & 0 \end{vmatrix} \times \begin{vmatrix} \theta_{12} \\ \theta_{13} \\ \theta_{41} \\ \theta_{23} \\ \theta_{42} \\ \theta_{43} \\ \varphi_1 \\ \varphi_2 \\ \varphi_3 \\ \varphi_4 \end{vmatrix} = \begin{vmatrix} b_{12} \\ b_{13} \\ b_{41} \\ b_{23} \\ b_{42} \\ b_{43} \\ 0 \\ 0 \\ 0 \\ 0 \end{vmatrix} \tag{4}$$

The matrix in equation (4) may easily be diagonalised and the equation solved in closed form by back substitution. In this example, the minimum number of extra equations (i. e. one) has been added to make it possible to solve for the imaginary parts of equations (2). Since the term "minimum redundancy" is sometimes used to mean non-redundant, the procedure of using the least redundancy that yields a closed form solution might reasonably be termed "critical redundancy". In refering to the solution of the imaginary parts of equations (2) one may be specific and refer to "critical phase redundancy".

If one now considers the real parts of equations (2), one finds that there is only one disposable parameter, corresponding to the gain of one of the antennae. Thus to solve the real parts of (2) in closed form requires a higher degree of redundancy than to solve the imaginary parts, specifically $N-1$ redundant spacings. For the example of Figure 3 it is not possible to give a simple scheme that results in "critical modulus redundancy".

In each case it is possible, under most conditions, to build into the instrument sufficient redundancy to produce an overdetermined system of equations and thus to find a least squares solution. It has already been shown [2] that redundant calibration leads to a reduction of error that permits the reconstruction of very high dynamic range images in radio astronomy.

Accurate determination of the phases $\theta(\xi)$ is usually more important in image reconstruction than is accurate determination of the $|\gamma(\xi)|$ values. Thus "critical phase redundancy" is more important than "critical modulus redundancy".

In the context of a satellite instrument the principle of redundancy has an added advantage. By building the instrument to provide an overdetermined system of equations one can ensure that the loss of output from one (perhaps more) of the apertures will not seriously reduce the number of ξ-values at which measurements are made. In a non-redundant N aperture system, loss of a single element in the array leads to a loss of measurements of $\gamma(\xi)$ at $N-1$ values of ξ, which could seriously damage the imaging capability of the instrument.

In principle, redundant calibration permits exact determination of the various g and $\gamma(\xi)$ values in equations (2). In practice, photon noise sets a limit below which noise in the system cannot be reduced. It can be shown, [6] that if the standard deviation in the b's of equations (2) is to be kept below σ radians, then the source under study must be brighter than:

$$(5) \quad m \sim 2.5\,(8+\lg[2\,A\,q\,\tau\,\Delta\lambda\sigma^2\,|T(\xi)|^2\,|O(\xi)|^2]),$$

where:

- A is the total collecting area in square metres;
- q is the instrument quantum efficiency (detector + optics);
- τ is the integration time in seconds;
- $\Delta\lambda$ is the bandpass in nanometres;
- $T(\xi)$ is the interferometer OTF, normalized such that $T(0)=1$;
- $O(\xi)$ is the object Fourier transform, normalized such that $O(0)=1$.

Taking possible values for a satellite instrument (OASIS):

- A $=9\ m^2$ (nine apertures, each of area lm^2);
- q $=0.01$ (optics 10%, detector 10%);
- τ $=1$ second (time constant for instrument stability);
- $\Delta\lambda$ $=100$ nm (broad band imaging, either by integration on the detector or *a posteriori* integration after dispersion);
- σ $=6.3\times10^{-2}$ rad ($\lambda/100$ accuracy);
- $T(\xi)$ $=0.11$ (reciprocal of number of apertures);
- $O(\xi)$ $=1$ (unresolved object),

one finds that the source must satisfy $m \lesssim 12.3$, even for unresolved sources. Despite the fact that there are, on average, approximately 30 sources brighter than this per square degree of sky, this is not a very satisfactory limit for an expensive instrument. However, since one would expect to find a source of this brightness within 0.5 degrees of almost any region of the sky, one might consider using such a source as a reference to stabilize the instrument during long integrations on an arbitrary object. A differential delay line of approximately 30 cm would be adequate to compensate for the path length difference over a 0.5 degree field and with an interferometer of 40 m baseline. Thus if one were to slice the image formed by each aperture (at the focal planes shown in Figure 1) and provide such a differential optical delay in the path-length compensation system for each aperture, it would almost always be possible to find a suitable reference source to permit one to achieve $\lambda/100$ accuracy in calibration whilst observing any region of the sky.

A further advantage of redundant calibration in the context of a satellite instrument is that a closed form solution is simple to hard-wire and this should be an advantage for real-time instrument calibration. Similarly, an over-redundant least squares is easily performed using a hard-wired systolic array.

If redundant calibration is to be used to compensate for atmospheric distortions the integration time used must be less than the time constant of the atmospheric turbulence (about 10^{-2} sec.). This leads to a reduction by 5 in the limiting magnitude, compared to OASIS performance. Further, the representation of φ as a constant means that, either each aperture will require active optics to correct the atmospherically distorted wavefront (which should not be prohibitively difficult for lm apertures), or each aperture must be much smaller than the wavefront correlation length (typically $\sim$ 10 cm). If each aperture were reduced to a 1 cm square, the limiting magnitude for path-length correction accurate to $\lambda/100$ would be $m \lesssim -2.3$. A Labeyrie-type array of 1 m dishes with active optics turbulence correction could have a limiting magnitude of $m \lesssim 12$ for $\lambda/10$ operation. However, the lack of isoplanatism of the atmospheric point spread function means that in this case it is not feasible to slice the image to provide a reference field. The next section will concentrate on OASIS.

5. OASIS-instrument overview

This instrument is not a finalised design, but represents a family of possible variations upon a particular theme that may be summarised as follows:

1. A two-dimensional array of collector apertures mounted on a single structure and using at least "critical phase redundancy".

As discussed previously, the central interferometer must encode the information in a non-redundant manner, in order that the interference between each aperture pair may be separately identified and measured. In order to facilitate spectral dispersion it is an advantage if the apertures are redistributed in such a way that the mutual inclinations all lie in the same plane, this ensures that all the interference fringes are parallel to each other. This basic concept is suitable for an instrument that could be launched as a single payload with present day launch vehicles and give baselines up to a maximum of 27 m (with the three arm scheme of Figure 4). However, the availability of space sta-

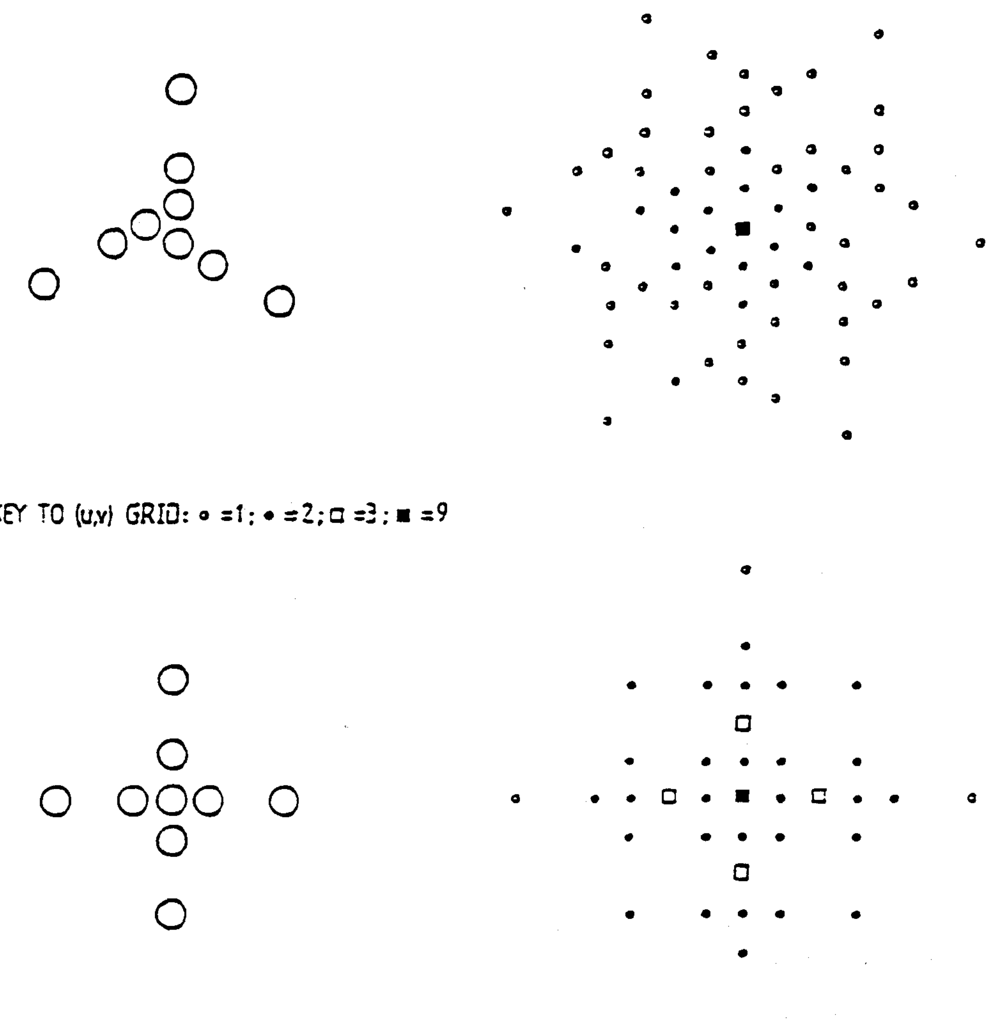

Fig. 4. — Two possible 9-aperture arrangements for OASIS, with their (u, v) sampling grids on the right. The number of times that a given (u, v) spacing is sampled is indicated by the key, the filled square is located at the origin. The upper sheme has "critical phase redundancy" and may be extended to longer baselines whilst preserving that feature. With all "critically redundant" schemes, if a redundant spacing lies on a null in the object spectrum, or if an interior aperture were deleted from the scheme, a one parameter solution would be left. The lower part of the Figure shows an arrangement that provides a greatly over-determined system, which thus allows least squares error reduction. The central aperture is the only aperture in this scheme whose deletion would obstruct the closed form phase and modulus solutions.

tion provides the possibility of greater baselines — if the three arm scheme is extended to 21 apertures, with 1 m as the smallest spacing between two apertures, the maximum overall baseline would exceed 100 m. The limit to the number of apertures depends upon interferometer design, 21 does not seem unreasonable.

2. Imaging slicing and path-length correction using optical trombones to facilitate broad-band imaging at two points up to half a degree apart on the sky. One of these points is then used to image a reference object from observations on which the instrument is calibrated/phase-locked to target accuracies of about $\lambda/100$ (i. e. to about 5 nm).

A further advantage of this is that the optical delay lines may be used to achieve fine guiding of the instrument, thus relaxing the constraints on the overall instrument pointing. Pointing control for individual apertures is quite relaxed, since a pointing error will simply lead to a change in fringe period. Naturally, such a change in fringe periods must not be so large as to cause confusion between the different fringes in the system.

Thus:

3. Measurement of both modulus and phase of the complex degree of coherence of the source under study in the long-time integration channel. Measurement of the phase to a few degrees accuracy should provide images with good dynamic range (100 : 1).

The redundant calibration scheme may, of course, be applied to the object under study in the long-time integration channel and thus provides the facility to compensate any constant but unexpected phase differences between the reference and object channels.

4. Fullest use of spectral information to provide images at a range of wavelengths, or to improve the signal to noise where there is no evidence of wavelength dependent structure.

The spectral resolution is not dictated by imaging requirements, since a resolution of 0.1 nm would already give a field of view greater than one second of arc at baselines in excess of 100 m. For broadband imaging one can, of course, integrate up after detection. A total working wavelength range of $100 \lesssim \lambda \lesssim 1\,000$ nm would be ideal, but it may not be possible to achieve full coverage of this wavelength range. A further advantage of using a range of wavelengths is that path-length errors can be measured over a greater range. If only a single wavelength is used path-length errors may only be measured to modulo λ (i. e. phase to modulo 2π).

It should be noted that in evaluating the limiting magnitude in the previous section, an integration time of 1 second was assumed for instrument calibration. This time will be limited by the vibration spectrum of the whole instrument in its space environment and this, in turn, cannot be carefully evaluated until a specific design is given. The crucial value here is the final value achieved for the product $q\tau\Delta\lambda$. A reduction by a factor of 10 in this product would reduce the limiting magnitude to 10, with a consequent reduction of density of suitable reference sources to 4 per square degree, at which point it must be assumed that significant regions of the sky would not be accessible to the long-time integration channel.

6. Discussion

In this paper we have examined the principles of "critically redundant calibration" and illustrated how it works by use of a simple example formulated in terms of matrix equations. We have indicated how one might use this principle and that of image slicing to construct a space-borne interferometer that should be capable of using one metre apertures to synthesise an equivalent aperture approaching 100 m diameter. The density of suitable reference sources means that this technique has, effectively, no limiting magnitude for the non-reference field. However, the structure and brightness of the non-reference source will affect the signal to noise ratio achieved on that object in a given observing time. Application to correction of atmospheric turbulence has also been considered and a limiting magnitude of ~ 12 has been inferred as the probable upper limit for that application, though this limit would correspond to relatively low dynamic range images. Since the method yields an image from each integration time, the averaging of several of these could be used to improve image quality.

This, of course, leaves many questions unanswered. Computer simulations are obviously required in order to assess the quality of images obtained using different aperture arrangements and under different noise conditions. This, combined with more structural information, particularly vibration spectra, is required to determine whether such a structure is affordable and whether it is likely to be an effective means of addressing the pertinent astronomical questions. Other possibilities, e. g. various possible aperture arrangements and use of singular value analysis instead of CLEAN-like algorithms for image processing, also clearly need examination. It is hoped to address these questions in the near future.

Acknowledgements

This work has been partially supported by NATO Research Grant No. 723/84.

Manuscrit reçu le 2 janvier 1985.

REFERENCES

[1] A. R. Thompson and L. R. d'Addario, *Synthesis Mapping*, NRAO, PO Box 2, Green Bank, WV 24944, October 1982.

[2] J. E. Noordam and A. G. de Bruyn, High dynamic range mapping of strong radio sources, with application to 3C 84, *Nature*, 299, 1982, pp. 597-600.

[3] A. H. Greenaway, Diffraction-limited pictures from single turbulence-degraded images in astronomy, *Optics Commun.*, 42, 1982, pp. 157-161.

[4] N. R. Arnot, A technique for obtaining diffraction-limited pictures from a single large aperture small exposure image, *Optics Commun.*, 45, 1983, pp. 380-384.

[5] A. H. Greenaway, J. G. Walker and J. A. G. Coombs, Ambiguities in speckle reconstructions – some ways of avoiding them, In *Indirect Imaging*, J. A. Roberts Ed., CUP, 1984.

[6] M. Born and E. Wolf, *Principles of Optics*, Pergamon Press, London, 1959.

[7] A. H. Greenaway, Estimation of log-modulus and phase of the Fourier transform of a photon-limited process, *Optics Commun*, 54, 1985, pp. 75-80.